Time-Dependent Photoionization Modeling of Warm Absorbers: High-Resolution Spectra and Response to Flaring Light Curves

Dev R Sadaula[1], Manuel A Bautista[2], Javier A Garcia[3], Timothy R Kallman[1]

[1] NASA Goddard Space Flight Center, 8800 Greenbelt Rd, Greenbelt, MD 20771, USA
[2] Western Michigan University, 1903 W Michigan Ave, Kalamazoo, MI 49008, USA
[3] California Institute of Technology, 1200 E California Blvd, Pasadena, CA 91125, USA

Abstract

The nature of the extreme variability of the central ionizing source in Active Galactic Nuclei (AGN) suggests that the outflowing gas may deviate from the commonly approached equilibrium approximation. Hence, we need to consider a time-dependent calculation to describe the ionization states and the transmitted spectra accurately. To see the effects of the variability quantitatively, we carried out a time-dependent photoionization simulation by solving a time-dependent balance equation for level population, internal energy, and radiative transfer simultaneously and self-consistently and developed a time-dependent photoionization modeling code (TDP code). The outflows responsible for the absorption of the X-rays, also known as warm absorbers, are investigated using this newly developed TDP code for various input parameters such as density, the shape of the incident light curve, SED, etc. We simulated the outflow for step and flare incident light curves. We analyzed the high-resolution transmitted model spectra to understand how the ionization structure of the outflow changes over time. The study of the time-resolved spectra could be used in constraining the warm absorber properties such as density and, in turn, the location. This will help to understand the AGN feedback by estimating the kinetic power of the outflow. In this poster, we present the results of how the warm absorber gas responds to the flaring incident ionizing radiation and the transmitted spectrum changes over time.

Introduction

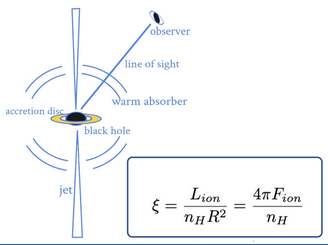

$$\xi = \frac{L_{ion}}{n_H R^2} = \frac{4\pi F_{ion}}{n_H}$$

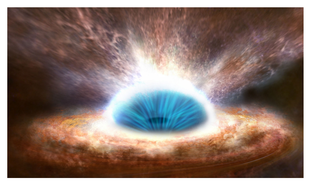

Dispersed outflow in AGN

- The top left figure is a cartoon (not to scale) showing various Active Galactic Nuclei (AGN) components.
- Most radiation is emitted from the accretion disc and corona, where gravitational potential energy is converted to mechanical and electromagnetic energy (Lynden-Bell, 1969). These seed photons are up-scattered in a high-temperature corona and converted into X-rays.
- Warm absorbers(WA) are outflowing X-ray-absorbing gas. The top right image is the artistic image of dispersed outflow.
- There is a large uncertainty in the location of WA. This yields uncertainty in what part of the outflowing gas the warm absorber carries. (Contribution to Feedback)
- The uncertainty comes from the degeneracy in density and location in the ionization parameter.

Variability in AGN

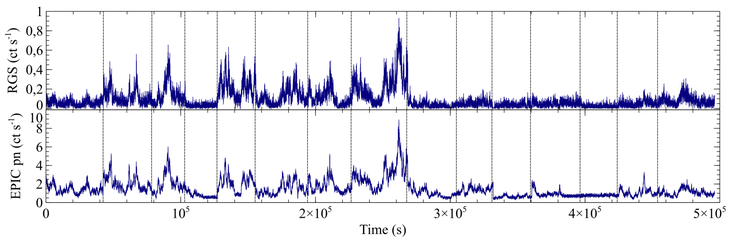

Silva et al. 2016

- RGS light curves for the 15−17 Å band (top) and EPIC-pn light curves for 1.5−10 keV (bottom) of NGC 4051. The dashed lines separate each individual observation. The flux varies by a factor of 4, 5, or more at a time scale of $\sim 10^4$ s.
- By modeling the incident light curve as a flare, we could calculate the density of the gas and other parameters based on how fast they respond.

Time-Dependent Photoionization

- It is common for photoionization models to assume the gas is in a steady state. Photoionization codes such as XSTAR (Kallman & Bautista (2001)), CLOUDY (Ferland et al. (1998)), and MOCASSIN (Ercolano et al. (2003)) all make the equilibrium assumption.
- The equilibrium assumption is valid only when the equilibrium time scale for the microscopic processes like excitation, ionization, and thermal balance is much shorter than the time scale of the variation of the ionizing source or the time scale of change in the geometrical shape of the plasma.
- If the ionizing flux changes at a rate faster than the microscopic equilibrium time scale or if the condition of the plasma changes shorter than those of the microscopic time scale, the state of the plasma departs from the equilibrium. In this situation, the time-dependent calculation needs to be considered.
- To carry out this time-dependent calculation, we numerically solved the time-dependent radiative transfer equation, level population equation, and energy balance equation.

Equations

$$\frac{dn_i}{dt} = \sum_{j=1}^{p} n_j R_{ji} - \sum_{k=1}^{p} n_i R_{ik}$$ Rate of change of level population

$$\frac{dT}{dt} = \frac{2}{3kn_t}(\Lambda - \Gamma - \frac{3}{2}kT\frac{dn_t}{dt})$$ Time-dependent temperature

$$\frac{1}{c}\frac{\partial L_\varepsilon(x,t)}{\partial t} + \frac{\partial L_\varepsilon(x,t)}{\partial x} = -\kappa_\varepsilon(x,t)L_\varepsilon(x,t)$$ Time-dependent radiative transfer

Where n_i and n_j are the level population densities in the unit of cm^{-3}, R_{ji} is the transition rate from all the j^{th} to i^{th} energy level, R_{ij} is the inverse of R_{ji} in unit s^{-1}, p is the number of energy levels for a neutral atom, T is the temperature (K), n_t is the number density of free particles (~electrons + protons), Λ and Γ are heating and cooling rates (erg s^{-1} cm^{-3}), c is the speed of light (m s^{-1}), L_ε ithe s specific luminosity of radiation field (erg s^{-1} erg^{-1}), κ_ε is the absorption coefficient (cm^{-1}).

- All these equations are solved simultaneously and self-consistently using ordinary differential equation solver DVODE and initial conditions calculated by standard XSTAR.
- Since the equations are stiff, an implicit method is used in solving these equations.

Model Parameters

- Density (n_H) = 10^7 cm^{-3}
- Column density (N_H) = 10^{22} cm^{-2}
- Low state flux (F1) = 6.5x10^7 erg s^{-1} cm^{-2}
- High state flux (F2) = 6.5x10^8 erg s^{-1} cm^{-2}
- Variability time of flare = 30,000 s
- Flux factor = 10
- Initial Source Luminosity (L) = 10^{44} erg s^{-1}

Light Curves (LC)

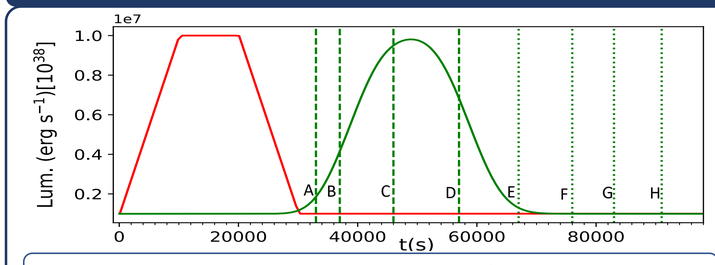

- The red line represents the incident light curve at the face, while the green curve represents the transmitted light curve after its propagation through the cloud (at the back of the cloud). A, B, C, and D are times during the flare. E, F, G, and H are times after the flare completely propagated through the cloud.
- The light curve becomes smoother when it propagates deeper into the cloud.

Ion Fraction Profiles for O VIII

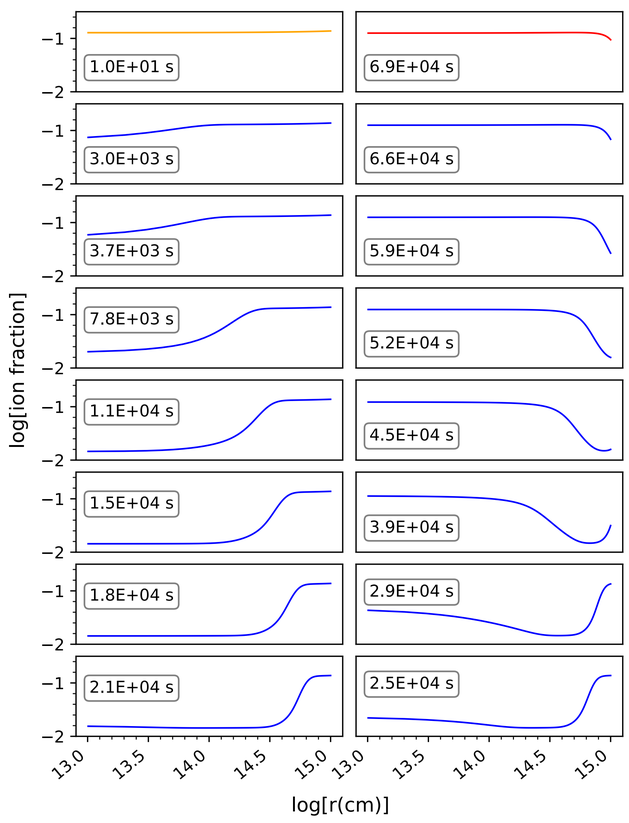

- The left column represents the ion fraction profile while the flux is going up, and the right column represents it while the flux is going down for the baseline model.
- The orange and red lines represent the initial and final low flux state ion fraction profile.

Ion Fractions vs. Time

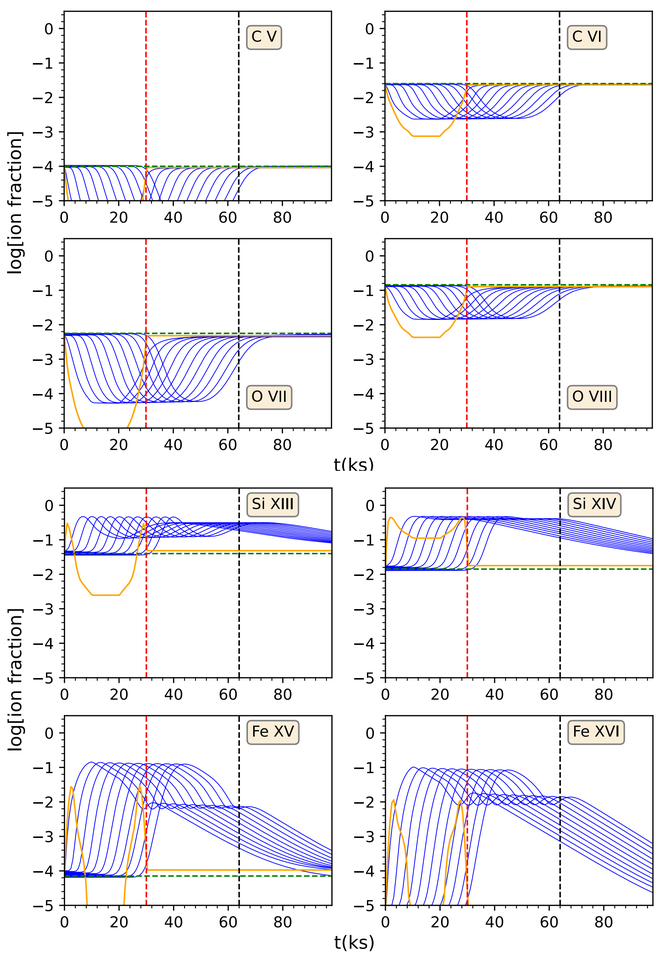

- All the above panels show the fractions vs. time at various locations in the cloud for some of the representative ions for this model. The red, black, and green dashed lines represent the variability timescale (30,000 s), the propagation time of flare (64,000 s), and the equilibrium ion fraction with a low flux state, respectively.
- The individual blue curve corresponds to a particular location in the cloud. The curve that evolves earliest is at the face of the cloud, and the one that evolves latest is at the back of the cloud. Orange curves represent the equilibrium ion fraction.
- The highly ionized ion has a comparatively longer time because of the successive formation and destruction of ions of a low ionization state.

Transmitted Spectra

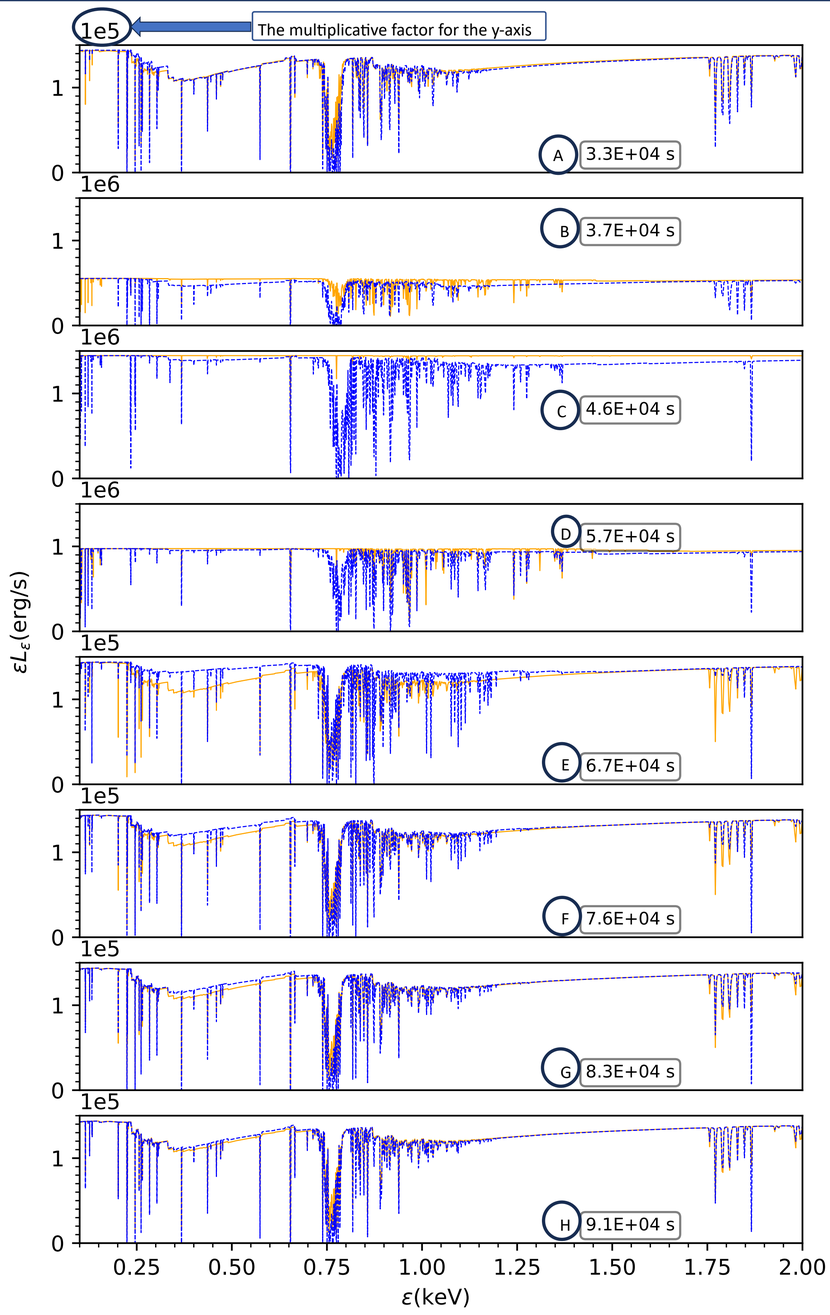

- All the above panels show the transmitted spectrum at a different time displayed in the box. The orange curves are instantaneous flux equilibrium spectra, and the blue are time-dependent spectra.
- The blue spectrum in the first panel corresponds to the initial low-state flux, represented by the first vertical dashed line in the light curve.
- The second panel corresponds to a point where the flux is rising (point B in LC)
- The third panel is when flux remains at a high state. (point C in LC)
- The fourth panel is at a time for flux going down. (point D in LC)
- The remaining panels correspond to times (E, F, G, H) after the flare propagated through the cloud.
- The spectral equilibration time in this energy interval is ~ 91 ks for this model.

Summary and Conclusions

1. Time-dependent effects can be important when the illuminating flux varies on timescales less than the ionization, recombination, and propagation timescales in warm absorber clouds. If so, photoionization and thermal equilibrium are invalid and will give misleading answers when fit to observations.
2. The microphysical timescales depend on the density and other things: the gas is more likely to remain near equilibrium at high density. At low density, the gas will not respond to changes in the illumination. At intermediate densities, simulations such as the ones shown here are needed.
3. Our previous work (Sadaula et al. 2023) presented models for simple step-up or step-down of the illuminating flux. Here we present models for flares.
4. Differing photoionization vs. recombination times, and thermal time, lead to complicated asymmetries in the time dependence of ion fractions vs. time.
5. Time-dependent radiative transfer causes the flare to propagate through the cloud at a speed slower than light speed; this is important quantitatively.
6. The time-dependent spectra are different from that of instantaneous flux equilibrium spectra.

References

- Ercolano, B., Barlow, M. J., Storey, P. J., & Liu, X. W. 2003, MNRAS, 340, 1136 doi: 10.1046/j.1365-8711.2003.06371.x
- Ferland, G. J., Korista, K. T., Verner, D. A., et al. 1998, PASP, 110, 761, doi: 10.1086/316190
- Garc ́ıa, J., Elhoussieny, E. E., Bautista, M. A., & Kallman, T. R. 2013, The Astrophysical Journal, 775, 8, doi: 10.1088/0004-637x/775/1/8
- Holczer, T., Behar, E., & Arav, N. 2010, ApJ, 708, 981, doi: 10.1088/0004-637X/708/2/981
- Holczer, T., Behar, E., & Kaspi, S. 2007, ApJ, 663, 799, doi: 10.1086/518416
- Kallman, T., & Bautista, M. 2001, ApJS, 133, 221, doi: 10.1086/319184
- Lynden-Bell, D. Galactic Nuclei as Collapsed Old Quasars. *Nature* 223**,** 690–694 (1969), doi: 10.1038/223690a0
- Rogantini, D., Mehdipour, M. , P., et al. 2022, Apj, 940, 122, doi: 10.3847/1538-4357/ac9c01
- Sadaula D., Bautista M., Garcia J., Kallman T., Apj, 946(93), 22 , doi : 10.3847/1538-4357/acbd40
- Silva, C. V., Uttley, P., & Costantini, E. 2016, A&A, 596, A79, doi: 10.1051/0004-6361/201628555